Nano Energy (2012) 1, 57–72

Available online at www.sciencedirect.com

SciVerse ScienceDirect

journal homepage: www.elsevier.com/locate/nanoenergy

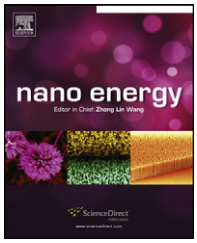

REVIEW

Nanomaterials and nanostructures for efficient light absorption and photovoltaics

Rui Yu, Qingfeng Lin, Siu-Fung Leung, Zhiyong Fan*

Department of Electronic and Computer Engineering, Hong Kong University of Science and Technology, Clear Water Bay, Kowloon, Hong Kong SAR, China

Available online 7 November 2011

KEYWORDS
Photovoltaics;
Nanomaterials;
Nanostructures;
Light trapping;
Carrier collection;
Low-cost

Abstract
Nanomaterials and nanostructures hold promising potency to enhance the performance of solar cells by improving both light trapping and photo-carrier collection. Meanwhile these new materials and structures can be fabricated in a low-cost fashion, enabling cost-effective production of photovoltaics. In this review, we summarize the recent development of studies on intriguing optical properties of nanomaterials/nanostructures and efforts on building solar cell devices with these materials and structures. As the family of nanomaterials has great diversity, we highlighted a number of representative materials and structures, including nanowires, nanopillars, nanocones, nanodomes, nanoparticles, etc. And we have covered materials include crystalline Si, amorphous Si, CdS, CdSe, CdTe, ZnO, $CuInSe_2$, etc. These materials and structures have different physical properties, such as band-gap, absorption coefficient, surface/bulk recombination rate, etc., as well as different synthesis/fabrication approaches. Works on these materials and structures have laid a solid foundation for developing a new generation photovoltaics.

Introduction

As a direct sunlight-electricity conversion phenomenon, photovoltaic (PV) effect was discovered close to one and half century ago. And PV technologies have experienced rapid development with the booming of semiconductor industry in the past few decades. However, up-to-date, PV generation only accounts for $<0.1\%$ electricity generation globally [1], mainly due to the fact that the existing PV technologies have yet not been able to produce electricity at a comparable price to that of convention generation methods, including firepower, hydropower, nuclear power, etc. In this regard, enormous amount of effort and resources have been invested on seeking new generation PV technologies, which can not only reach grid parity, but also replace fossil fuel based generation together with other means of renewable energy generation, to address environmental issues.

While the working principle of *p-n* junction type PV devices has been well understood for decades, material and device structure innovation has become the cutting-edge of the related research currently. Specifically, recent extensive studies have shown that by fabricating conventional semiconductor materials into nanostructures, particularly three-dimensional (3-D) arrays of nanostructures, such as nanowires

*Corresponding author. Tel.: +852 2358 8027.
E-mail address: eezfan@ust.hk (Z. Fan).

2211-2855/$ - see front matter © 2011 Elsevier Ltd. All rights reserved.
doi:10.1016/j.nanoen.2011.10.002

(NW) [2,3], nanopillars (NPL) [4,5], nanocone [6], etc., both photon absorption and photo-carrier collection efficiencies can be significantly improved [2,6–9]. In fact, the 3-D arrays of these nanostructures resemble natural form of light harvesting structures, botanical forests, to a fairly large degree but at a much smaller scale. Besides nanoscale structural engineering, unique nanomaterial physical properties, e.g. large surface-to-volume ratio [10,11] and quantum confinement [7,12], are being actively explored to enable PV with new mechanisms, including dye-sensitized solar cells, quantum dot solar cells, etc. In this review, we will summarize recent progress on aforementioned research directions. Specifically, we will begin with a brief review on theoretical and experimental studies on efficient light absorption and carrier collection with nanostructures. These studies cast a solid ground for nanostructured solar cells. Then we will review state-of-art research on PV devices fabrication and characterization with single and arrayed nanomaterials, mainly including NWs and NPLs. These concept-proof works have demonstrated feasibility of realization of cost-effective solar cells based on nanomaterials. Thereafter, the intriguing studies on quantum dot/nanoparticle solar cells will be reviewed. These nanomaterials can potentially enable new PV mechanism, e.g. multiple-exciton-generation (MEG). Meanwhile, these materials are compatible with solution-based processes, indicating their promising potential for low-cost PV. In the end, we will briefly review some of the unique nanostructures for solar cells, including nanodome, nano-forest, nanotube, etc. These studies can inspire more multi-dimensional research on nanostructured PV.

Enhanced performance with nanostructures

As a photoelectric device in nature, performance of a PV device largely relies on both photon absorption and photo-carrier collection. Therefore, in design of a PV device with decent energy conversion efficiency, both factors have to be optimized. Nevertheless, the requirements to optimize optical absorption and carrier collection can be in conflict. For example, in a planar structured solar cell, thicker materials is needed in order to achieve sufficient optical absorption; however, it will lower carrier collection probability due to the increased minority carrier diffusion path length, and vice versa. In fact, recent studies have shown that 3-D nanostructures can not only improve light absorption utilizing light trapping effect, but also facilitate photo-carrier collection via orthogonalizing the directions of light propagation and carrier collection. Progress on these studies will be summarized in the following section of the review.

Improvement on optical absorption: theoretical investigations

3-D arrays of nanostructures have gained tremendous attention in the field of photovoltaics, as absorption of sunlight in solar cells can be enhanced drastically by light trapping and carrier collection efficiency can be improved as well. Recently, optical absorption of nanostructure arrays have been extensively explored by many research groups, aiming at acheiving optimzed optical design for efficient solar cells [2,6,13–15]. In fact, optical properties of engineered 3-D nanostructues can be theoretically simulated using a number of tools, and the theoretical understanding of the device optical performance can greatly facilitate rational design and implement optimal PV structures. In particular, Chen and the co-workers reported the numerical modeling of optical absorption of periodic nanostructures including silicon NW arrays, nanohole arrays and nano-pyramid arrays [16–18]. The schematics of the periodic NW structure is shown in Fig. 1a. The effects of NW diameter, length, and filling ratio on the optical absorption of NW arrays were systematically analyzed using transfer matrix method (TMM) [16]. Calculations showed that the electromagnetic interaction between NW cannot be neglected, and nanowire structures showed higher absorption than their thin film counterparts, particularly at high-frequency regime, as shown in Fig. 1b [16]. On the other hand, at low-frequency regime, nanowire arrays absorb less due to small extinction coefficient and low material filling ratio, which can be improved using unique nanostructure engineering discussed in the following section.

Han and Chen furthered their work by investigating silicon nanohole arrays as complementary light harvesting structures and compared them to nanorod (NR) arrays, as shown in Fig. 1c [17]. Simulation results showed that absorption at λ=670 nm increases as the filling fraction decreases in both nanohole and NR arrays as a result of the smaller optical density, which creates antireflection effect. Moreover, nanohole arrays show better optical absorption than NR arrays over the entire range of the investigated filling fraction, which is attributed to both effective light coupling as well as the large density of waveguide modes [17].

In many cases, light trapping is the effect of increasing optical path of photons inside nanostructures by Lambertian scattering, which has a theoretical limit of $4n^2$ where n denotes the refractive index of the material [18]. Recently, Han and Chen examined light trapping in thin silicon nanostructures for solar cell applications (Fig. 1d) [18]. Using group theory, they design a nonsymmetric tapered two-dimensional gratings structure, which shows absorption close to the Lambertian limit at normal incidence. Furthermore, they demonstrated that rod array structures with nonsymmetric tapered tops can exhibit absorption close to the Lambertian limit even when averaged over all directions of incidence. These effects indicate a possibility to reduce thickness of crystalline Si wafer by 2 orders of magnitude while maintain the same optical absorption capability [18].

Improvement on optical absorption: experiments

Besides theoretical analysis, many experimental works have been done to fabricate 3-D nanostructures and characterize their unique optical properties. In general, the fabrication methods for the arrayed nanostructures can fall into two major categories: top-down and bottom-up approaches. Top-down approaches mainly refer to those that rely on lithographic patterning, or etching materials to shape nanostructures [2,6,19–21]. On the other hand, bottom-up approaches refer to those methods involving growing/assembling nanomaterials from atomic scale, for example, vapor-liquid-solid (VLS) growth [22–26], vapor-solid (VS) growth [27,28], electrochemical growth [29,30], etc. In practice, top-down approaches can be used to fabricate well-defined nanostructures; however, the fabrication cost

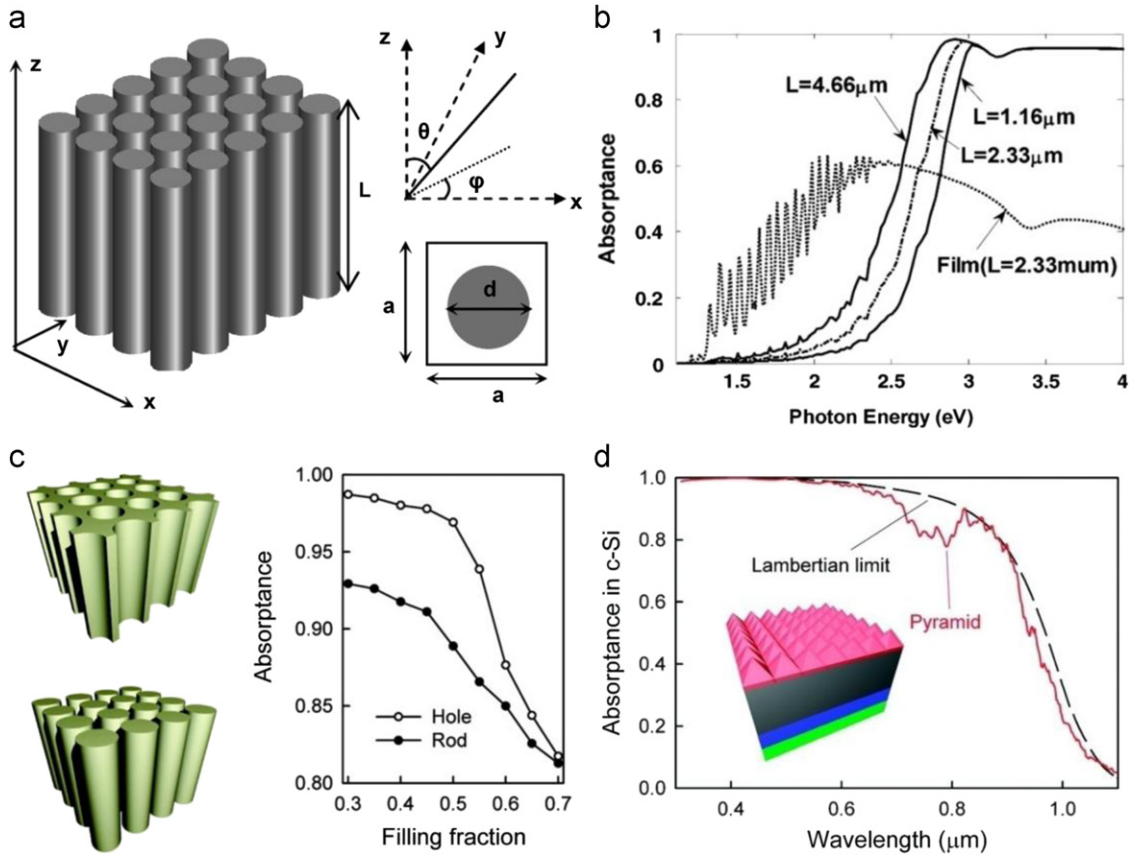

Figure 1 (a) Schematic drawing of the periodic silicon nanowire structure. The parameters are the length L, the period *a*, and the diameter *d*. In the figure, θ and ϕ are the zenith and azimuthal angles, respectively. (b) Absorptance of nanowires with various filling ratios obtained by TMM and the Maxwell-Garnet approximation. Adapted with permission from Ref. [16]. (c) Schematic illustrations of nanohole and NR arrays. Adapted with permission from Ref. [17]. (d) Absorptance of a pyramid structure. Red solid line represents absorptance of a pyramid structure. Black dashed line represents the Lambertian limit of a c-Si film of equal thickness. Adapted with permission from Ref. [18].

is typically high. On the other hand, bottom-up growth methods yield diverse nanostructures at relatively low cost, in some cases the shape of the nanostructures can be also well controlled [4,8,31,32]. In the following paragraphs, several representative works on 3-D nanostructure fabrication and optical property investigation will be introduced.

Since Si is the dominant material in PV industry, fabrication and characterization of Si based nanostructures has been extensively studied. As shown in Fig. 2a, Garrnett and Yang fabricated a perfectly ordered Si NW array using self-assembly of silica beads followed by deep reactive ion etching (DRIE) on a Si wafer [2]. The excellent packing shown in the SEM images can extend over large areas, up to 10 cm^2, limited only by the size of the dip-coating cell and wafer. Optical transmission (Fig. 2b) clearly shows that the NW arrays reduce the intensity of the transmitted light compared to the planar control sample, indicating a strong light-trapping effect [2]. Moreover, light-trapping path length enhancement factor, defined as the apparent optical thickness of the structure divided by its actual thickness, was estimated to be increased by 73 times for the SiNW array films in the AM1.5G spectrum, even higher than the previously mentioned Lambertian light trapping limit, due to the photonic crystal enhancement effects in the devices [2].

Certainly 3-D Si NW arrays can be achieved by etching Si wafers, using dry etching and solution based electroless etching [2,33]. Large effort has been invested on growing Si NW arrays from bottom-up. Fig. 2c demonstrates ordered Si NWs grown vertically using a typical catalytic VLS process [15]. Research has shown that although such a NW array has less than 5% areal fraction of wires, it can achieve up to 96% peak absorption, and up to 85% of day-integrated, above-bandgap direct sunlight absorption (Fig. 2d) [15]. Using AM 1.5D spectrum at normal incidence, the enhanced infrared absorption of the Si wire array yielded a greater overall absorption of above-bandgap photons than the equivalently thick, ideally light-trapping planar absorber [15]. In fact, taking all measured incidence angles into account, the day-integrated absorption of the wire array (A_{avg}=0.85) slightly exceeded that of the planar light-trapping case (A_{avg}=0.82). Thus, the Si wire-array geometry can enable solar cells that reach, and potentially even exceed, the theoretical absorption limit, per volume of Si, of ideal light-trapping within a conventional planar geometry.

In another work, rather than using the top-down lithographic method and epitaxial wafer to obtain regular arrays of wire, Ge NPLs were assembled in the anodic alumina membrane (AAM) via catalytic VLS growth method, while the

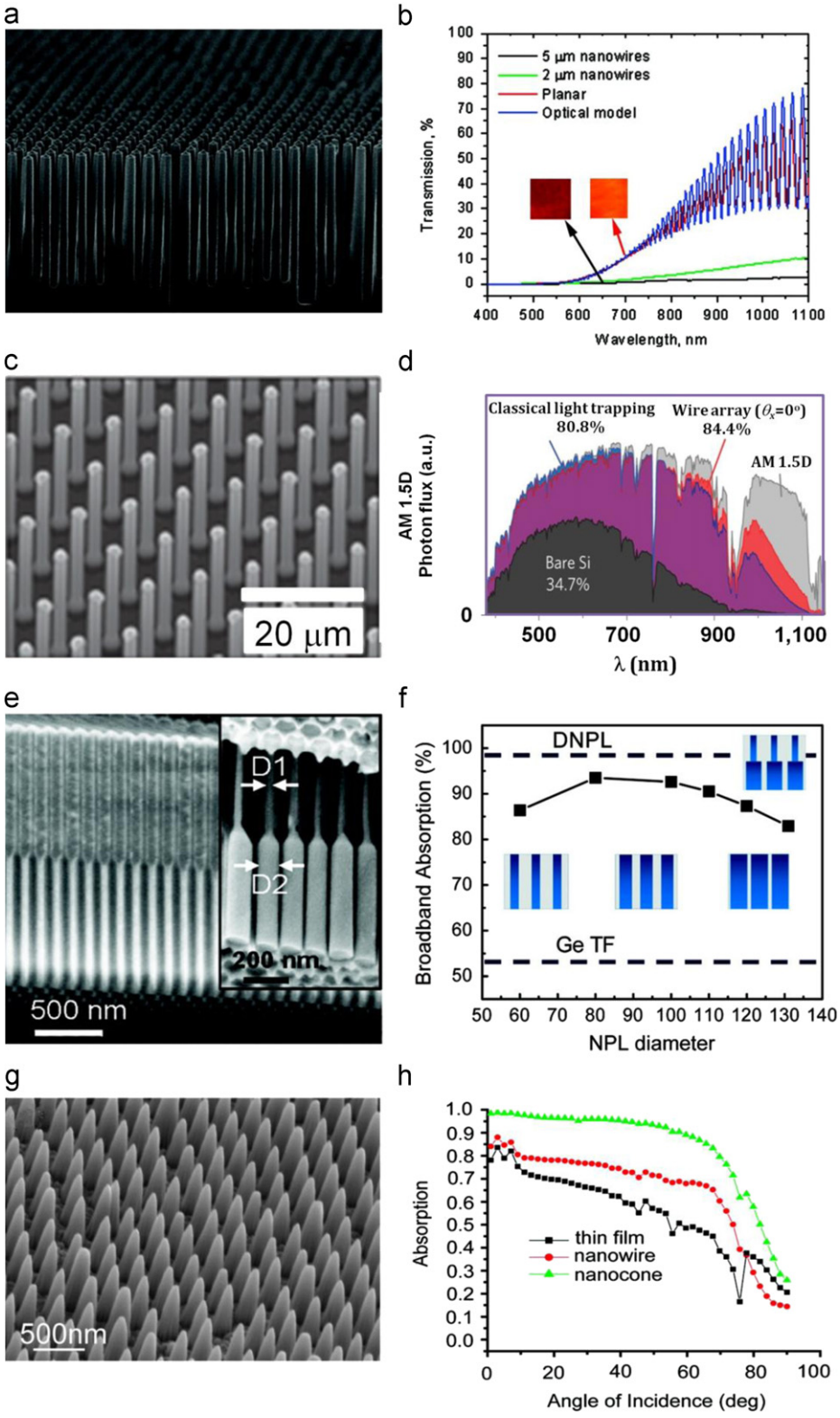

Figure 2 (a) SEM image of an ordered silicon NW array made by bead assembly and deep reactive ion etching. (b) Transmission spectra of thin silicon window structures before (red) and after etching to form 2 μm (green) and 5 μm (black) nanowires with the insets of backlit color images of the membranes before and after etching. Adapted with permission from Ref. [2]. (c) SEM image of Si wire arrays grown by a photolithographically patterned VLS process. (d) Illustration of the normal-incidence, spectrally weighted absorption of the AM 1.5D reference spectrum of the Si wire array. Adapted with permission from Ref. [15]. (e) SEM image of a blank AAM with dual-diameter pores and the Ge DNPLs (inset) grown by VLS method. (f) Average absorption efficiency over λ=300–900 nm for single-diameter NPLs as a function of diameter compared with that of a DNPL array with D1=60 nm and D2=130 nm. Adapted with permission from Ref. [8]. (g) SEM image of a-Si:H nanocone arrays prepared by Langmuir–Blodgett assembly and etching technique. (h) Absorption of ITO/a-Si:H samples with a-Si:H thin film, nanowire arrays, and nanocone arrays as top layer over different angles of incidence at wavelength λ=488 nm. Adapted with permission from Ref. [6].

AAM was fabricated by simply multiple-step etching and anodization [8]. In order to enhance the broad-band optical absorption efficiency, the researchers presented a novel dual-diameter nanopillar (DNPL) structure, as shown in Fig. 2e, which has a small diameter tip for minimal reflectance on the top and a large diameter base for maximal optical absorption once photon enters the NPL array [8]. Compared to the Ge blank film with only ~53% broad-band light absorption (Fig. 2f), the Ge NPL array has already achieved a much improved (~99%) broad-band optical absorption [8]. Note that the thin Ge nanopillars are partially exposed on the top and there is a smooth structural transition from small diameter segment to the large diameter part, thus this unique structure has a close to gradual change of effective refractive index from top to bottom, leading to excellent light absorption capability.

The above discussed photonic nanostructures are made of single crystalline materials, either by etching crystalline raw material or catalytic bottom-up growth. In addition, 3-D nanostructures made of amorphous materials are also of particular interest as anti-reflective layers for solar cells. As an example, Zhu et al. fabricated a-Si:H NWs and nanocones using wafer-scale Langmuir–Blodgett assembly and etching technique [6]. Fig. 2g shows a SEM image of a-Si:H nanocone arrays after RIE. The length of each nanocone is ~600 nm. The tip diameter is ~20 nm while the base diameter is ~300 nm. These a-Si:H nanocone arrays have shown greatly enhanced absorption compared to their thin film and NW arrays counterparts over a large range of wavelength and angles of incidence, due to the gradual reduction of the effective refractive index away from the surface leading to superior antireflection properties. More than 90% of light is absorbed at angles of incidence up to 60° for a-Si:H nanocone arrays, while NW arrays and thin films only absorb 70% and 45% of the light (Fig. 2h). In addition, the absorption of nanocone arrays is 88% at the band gap edge of a-Si:H, which is much higher than that of NW arrays (70%) and thin films (53%) [6].

Improvement on photo-carrier collection

Light absorption and photo-carrier collection are two key aspects of an efficient PV device. Besides enhancing photon capturing capability, well designed nanostructures can also improve photo-carrier collection. In particular, short collection lengths can facilitate the efficient collection of photogenerated carriers in materials with low minority-carrier diffusion lengths. In this regard, Spurgeon et al. proposed a PV device structure consisting of vertically aligned arrays of radial *p-n* junction nanorod solar cells [34]. As shown in Fig. 3a, each NR in the array has a shallow *p-n* junction acting as a tiny solar cell, in which photoexcited minority carriers only have to travel across a short pathway to reach the charge-separating junction. Such a rod geometry device allows high carrier-collection efficiency even using low-quality films, leading to lower material cost in PV cells. This configuration relieves the competition between photon absorption and carrier collection, and open up the design space for further optimization. Following this principle, many NW solar cell architectures have been developed to orthogonalize the light absorption and carrier collection directions [4,15,34].

Nanostructure/materials based PV devices

Fundamental understanding of photon capturing and photo-carrier collection has paved the way for building cost-effective PV devices using nanostructures and nanomaterials. In this section, progress on PV devices base on a variety of nanostructures, including NWs, NPLs, nanotubes, nanoparticle, etc., will be reviewed.

NW/NPL based PV devices

Single NW PV devices

Quasi-one-dimensional materials, such as NW, NPL, nanotubes, etc., have been extensively investigated as nanoelectronic and

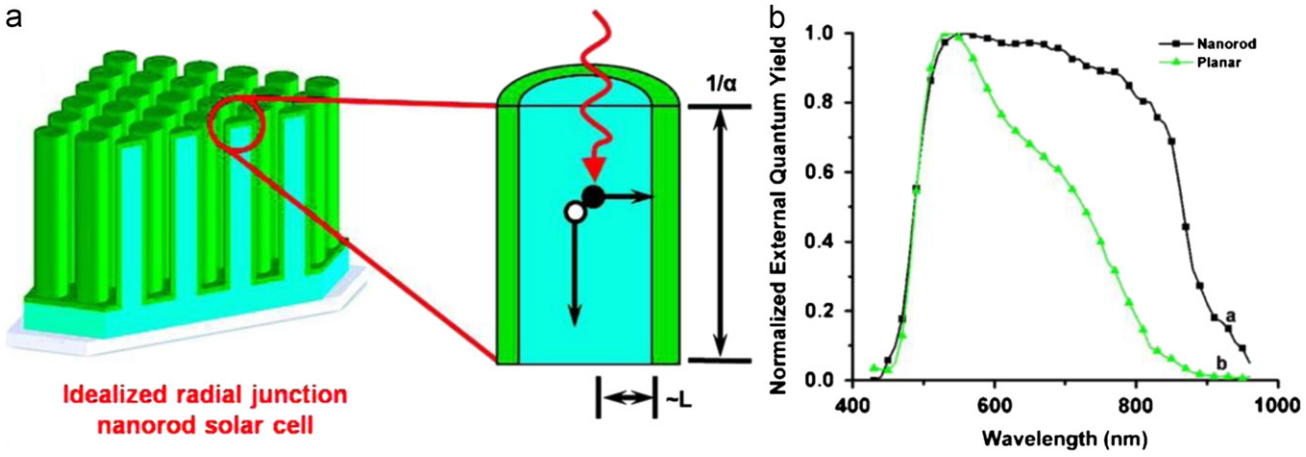

Figure 3 (a) Schematic cross-section of the radial *p-n* junction nanorod solar cell and a single nanorod. Such kind of structure does not require the collection length to be too long because they can absorb light in the axial direction while collecting charge carriers in the radial direction. The green area is *n*-type, and the blue area is *p*-type. (b) Normalized external quantum yield of photoelectrochemical cells with planar electrode (green line) and nanorod array electrode (black line). The quantum yield of the nanorod array electrodes at wavelengths greater than 600 nm decreased less than that of the planar electrodes. Adapted with permission from Ref. [34].

nano-optoelectronic materials due to fast and controllable carrier transport along the long axis. In fact, such property can also be utilized to achieve efficient photo-carrier collection as discussed previously. In order to understand PV effect at nanoscale, single NW PV devices have been fabricated and investigated. Particularly, a series of ground-breaking works on single NW PV devices has been done, in which core-shell and axial *p-n*/*p-i-n* junctions were realized on Si NWs for PV devices [35,36]. Due to large surface-to-volume ratio of NWs and high surface recombination of Si [37], the axial junction Si NW PV devices showed relatively low efficiency [36]. Nevertheless, core-shell structure with radial *p-n* junction demonstrated improved carrier collection efficiency and improved conversion efficiency up to 3.4% at 1 sun illumination and 4.8% at 8 sun condition [35]. Meanwhile, a single NW PV device was demonstrated as the power source for nanoscale pH sensor and logic circuits [35].

As Si has high surface recombination velocity [37], it is preferable to fabricate Si wires with large diameter to reduce surface-to-volume ratio, with passivation layer on wire surface to reduce surface recombination. On the other hand, it has been found that Au catalyst used in conventional Si NW vapor-liquid-solid (VLS) growth introduces impurity state in band-gap deteriorating minority carrier life-time and device performance [38]. In this regard, Kelzenberg et al. utilized Cu to catalyze Si microwire (MW) growth, and fabricated single-wire radial *p-n* junction solar cells with amorphous silicon and silicon nitride surface passivation coatings [39]. Such solar cell devices have achieved up to 9.0% apparent photovoltaic efficiency, with an open-circuit voltage of up to ~600 mV and fill factor over 80% [39]. Fig. 4a shows the schematic structure of the PV device showing a combination of radial and axial carrier collection scheme. Fig. 4b plots the current-density versus voltage (*J-V*) behavior of the most efficient device of each surface coating type. It can be seen that long minority-carrier collection length and reduced reflectivity of the a-SiN_x:H-coated devices consistently yielded the highest short-circuit current densities, up to 26 mA cm^{-2}, and resulted in the device with the greatest apparent photovoltaic efficiency up to 9.0%.

As several II-VI group compound semiconductors have much smaller surface recombination velocity than Si [37], recently, core-shell NW PV device made of II-VI group compound semiconductors were demonstrated by Tang et al. [40]. Fig. 4c shows a scanning electron microscopic (SEM) image of a PV device with a CdS NW core and Cu_2S shell. The CdS NW was grown with a catalytic VLS process [41] and Cu_2S shell was formed by partially exposing CdS NW to 0.5 M CuCl solution. To realize carrier collection, proper metal contacts were fabricated on CdS and Cu_2S shell precisely [40]. Fig. 4d shows the current-voltage (*I-V*) curve of such a PV device, demonstrating an open circuit voltage (V_{oc}) of 0.61V with an attractive fill factor (FF) over 80% and an energy conversion efficiency of ~5.4% under AM 1.5G illumination. It is worth noting such a CdS/Cu_2S NW PV device outperformed their thin film counterpart, mainly due to high quality of heterojunction and better carrier collection efficiency [42].

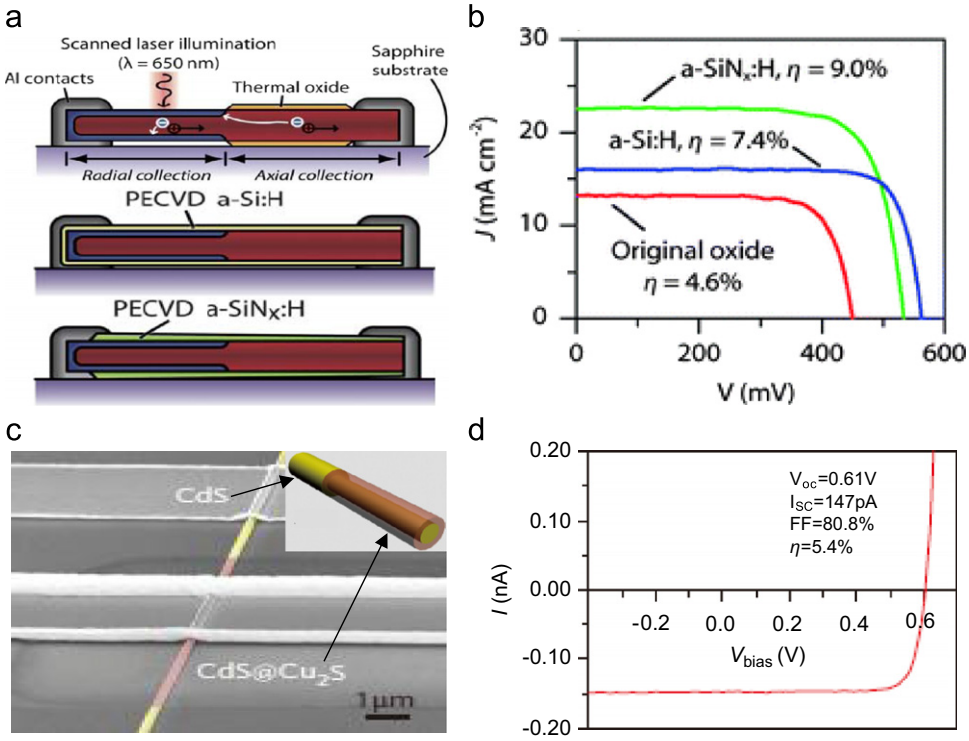

Figure 4 Single NW PV devices. (a) Schematic of wires without surface passivation (top) and with surfaces passivated by a-Si:H (middle) and a-SiN_x:H (bottom). (b) Photovoltaic *J-V* characteristics of the champion single-wire test structures of each surface passivation type. The current density of each device was normalized to the total non-shaded wire area (determined by SEM) to determine apparent photovoltaic efficiency. Adapted with permission from Ref. [39]. (c) Schematic and SEM image of a PV device; CdS and Cu_2S are highlighted with yellow and brown false colors, respectively. (d) *I-V* characteristic of a core-shell nanowire under 1 sun (AM 1.5 G) illumination. Adapted with permission from Ref. [40].

NW/MW/NPL array PV devices

Investigations on single NW PV devices provide us with fundamental understanding of the nanoscale PV effect. Meanwhile, these nanoscale solar cells can be potentially used to drive the nanoelectronic components [35]. On the other hand, arrays of these nanomaterials are needed for large scale PV generation, not mentioning the was improved photon capturing and photo-carrier collection capability associated with 3-D array structures.

Up-to-date, a number of works on NW/MW/NPL array-based PV devices using Si, InP, CdS, GaAs, ZnO, etc., as active materials have been reported [2,4,5,15,43]. And these structures have been fabricated with several approaches, including VLS growth [39,44–46], dry/wet etching [2,5,47,48], etc. Fig. 5a1–a3 demonstrates realization and characterization of a high efficiency Si wire array solar cell grown by VLS process [39]. Specifically, ordered arrays of *p*-type crystalline Si MWs were grown on Si(1 1 1) wafers with Cu as the metal catalyst [49]. After growth, the Cu catalyst was chemically removed. Radial *p-n* junctions were then selectively formed on the upper portion of each wire by thermal phosphorus diffusion, using a polymer (PDMS) etch-mask to define a SiO_2 diffusion barrier over the lower portion of each wire. As mentioned before, the radial *p-n* junction can improve photo-carrier collection, and such a fabrication process produced Si wires with radial *p-n* junction on one end and *p*-type core exposed on the other end to assist device fabrication. Fig. 5a2 shows tilted angle view of SEM images of a MW array. In fact, single wires from an array were fabricated into PV devices (Fig. 4a) and the characterization results were discussed before, shown in Fig. 4b [39]. Based on the measurement of single wire PV device, efficiency of arrayed Si wire PV device was projected to be 17.4%, as shown in Fig. 5a3 [39]. This work pointed out a future direction for high efficiency Si wire solar cells.

Besides using VLS to grow Si wires, there have been a number of reports on using top down etching to fabricate Si wire arrays for PV devices [2,5,47,48]. Recently, Kim et al.

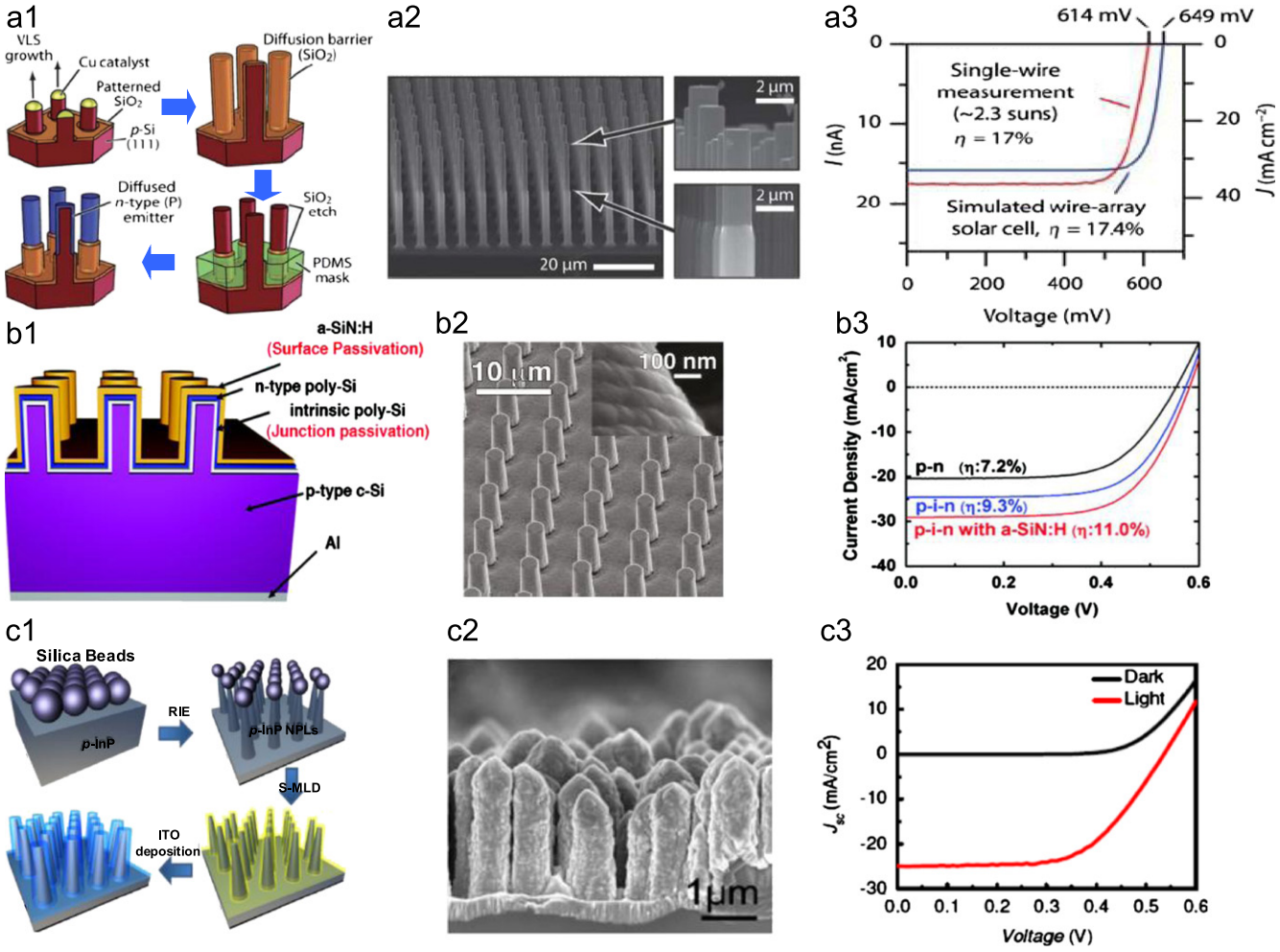

Figure 5 NW/NPL array PV devices. (a1) Fabrication process of Si wire solar cells. (a2) SEM images of a MW array following the fabrication step depicted in (a1), viewed at ~45° tilt (left) and ~90° tilt (right). (a3) Predicted efficiency and *J-V* characteristics of the wire-array solar cell. Adapted with permission from Ref. [39]. (b1) Schematic of the hybrid Si MW-planar solar cells. (b2) SEM images of the hybrid Si MW-planar solar cells. Inset: The coating of the poly-Si layers and the a-SiN:H layer is uniform. (b3) The light *J-V* curves of the best hybrid Si MW-planar solar cells with three different structures. Adapted with permission from Ref. [47]. (c1) Fabrication process of InP NPL solar cells. (c2) SEM images of NPLs coated with ITO (~100 nm thick). (c3) Photovoltaic *J-V* characteristics of InP NPL solar cells. Adapted with permission from Ref. [5].

reported an efficient Si MW (radial junction) solar cell fabricated by simple one-step photolithography, dry etching, and intermediate temperature deposition processes (Fig. 5b1) [47]. It showed that maximum efficiency was improved from 7.2% to 11.0% under AM1.5G illumination by passivating the top surface and *p*-*n* junction with thin a-SiN:H and intrinsic poly-Si films, respectively. The SEM image of a typical hybrid Si MW-planar solar cell with evenly spaced and vertically aligned SiMWs is shown in Fig. 5b2. The coating of the poly-Si layers and the a-SiN:H layer is uniform and conformal, as shown in the inset of Fig. 5b2. The photovoltaic properties of the hybrid Si MW-planar solar cells in Fig. 5b3 shows that the hybrid Si MW-planar solar cells with both the intrinsic and a-SiN:H layers exhibit a maximum efficiency of 11.0% (V_{oc} of 0.580 V, short circuit current density (J_{sc}) of 29.2 mA cm^{-2}, and FF of 0.649).

Besides using Si as material, Cho et al. have reported InP NPL solar cells with highly abrupt and heavily doped emitter layers fabricated using a sulfur molecular monolayer doping (S-MLD) scheme [5]. The fabrication process of the InP NPL solar cell is shown in Fig. 5c1. Monodispersed silica beads were spin-coated on the front side of a *p*-InP (1 0 0) wafer, followed by a two-step reactive-ion etching (RIE) to etch InP. Conformal surface n-doping of InP NPLs was achieved by the use of the S-MLD technique. Then indium tin oxide (ITO) was sputtered and annealed using rapid thermal annealing as the top contact. Fig. 5c2 shows the SEM image of a fully fabricated InP NPL cell. Under AM 1.5G illumination, the InP NPL cells obtained an efficiency of ~8.1%, with a V_{oc} of 0.54 V, J_{sc} of 25 mA cm^{-2} and FF of ~60% (Fig. 5a3) [5].

CdS NPLs/CdTe thin film PV devices

For NW/NPL based PV devices made of Si, GaAs, etc., the dominant carrier loss mechanism is surface recombination due to the high surface area to volume ratio [37,50]. Although Si and GaAs NW arrays have been extensively explored for PV studies, they are in fact not the best choice for the nanostructured solar cells for their relatively high surface recombination velocities [37]. Specifically, the reported surface recombination velocities of both non-passivated planar silicon and gallium arsenide structures have exceeded 10^6 cm s^{-1} [51–53]. This partially explains the reason that PV devices based on large dimension microwires of Si have demonstrated much more promising performance than those made of thin MWs [39]. As it has been shown previously, individual II–VI compound semiconductor nanomaterial has potential to deliver higher performance than its thin film counterpart [40]. In fact, typical cadmium sulphide (CdS) and cadmium telluride (CdTe) thin films have the untreated surface recombination velocities around 10^3 and 10^4 cm s^{-1}, respectively, which are 2 order of magnitude lower than those of Si and GaAs, making these material systems favorable for nanostructured solar cells [54,55].

In this regard, Fan et al. have fabricated CdS NPL/CdTe thin film hybrid solar cells utilizing anodic alumina membranes (AAMs) as templates [4]. A schematic fabrication process flow of the CdS NPL solar cells is shown in Fig. 6a. Highly ordered hexagonal pore array in an AAM was grown by a nanoimprint assisted anodization process [4]. CdS NPLs were then synthesized from the bottom of pores via the Au-nanoparticle catalyzed VLS growth method. The processed AAM was partially and controllably etched to expose the tips of the n-type CdS pillars to form the 3D structures. Thereafter, a *p*-type CdTe thin film with ~1 μm thickness was deposited by chemical vapor deposition to serve as the photoabsorption layer. The top electrode was finally metalized by the thermal evaporation of Cu/Au (1 nm/13 nm) in order to achieve an acceptable transparency and to form an ohmic contact with the *p*-type CdTe film. The backside electrical contact to the *n*-type CdS NPLs was simply the aluminum supporting substrate [4].

Electrical characterization of the NPL solar cell under different illumination intensities, ranging from dark to 100 mW/cm^2 (AM 1.5G), was shown in Fig. 6b. Under AM 1.5G illumination, a typical cell produced J_{sc} of 21 mA cm^{-2}, V_{oc} of 0.62 V, FF of 43%, and efficiency of 6%, which was found mainly limited by transmittance of top contact [4]. Interestingly, it was found that this NPL solar cell fabrication scheme can also be implemented on the bendable plastics for flexible PV applications. As shown in Fig. 6c, the entire NPL solar cell is sandwiched and embedded within the flexible PDMS [4]. Notably, due to the fact that the active material in the cell was located in the neutral mechanical plane of the PDMS substrate, it largely minimized the strain on the active cell elements, CdS NPLs. It is also demonstrated that a plastic NPL PV module almost shows same cell performance upon bending within a reasonable range.

Nanoparticle/quantum dot solar cells

As another major class of nanomaterials, nanoparticles have also been extensively studied for PV applications. The motivations of the related research rest in (1) small nanoparticles, or quantum dots (QD), have unique physical properties, such as size dependent band-gap [56–58], multiple-exciton-generation (MEG) [59], which enables new PV mechanism to potentially break current thermodynamic limit; (2) many nanoparticle synthesis are compatible with solution-based processes, therefore, PV fabrication based on these nanoparticles can potentially utilize high throughput, low temperature and low cost processes, such as ink-jet printing [60]. In this section, progress on both of these two interesting aspects will be reviewed.

Multiple-exciton generation enabled new concept solar cell

In conventional PV theory, one photon with above band-gap energy can only excite one electro-hole pair; therefore, the internal quantum yield will never exceed unity. And thus the thermodynamic limit sets the highest possible efficiency for a single junction solar cell to 33% [61]. In such case, additional energy from high energy photons will be converted to thermal energy of excitons, due to energy conservation. And this thermal energy will not be harvested by a conventional PV device thus will be wasted. It is logic to propose a ‘‘multiple-exciton generation (MEG)’’ process, in which one high energy photon excites two or more low energy excitons, still conserving total energy. In fact, such a scenario can be realized in quantum dots due to the discrete energy levels [12,62]. Specifically, in bulk semiconductors, inelastic carrier-phonon scattering leads to fast dissipation of the extra thermal energy of high energy excitons. However,

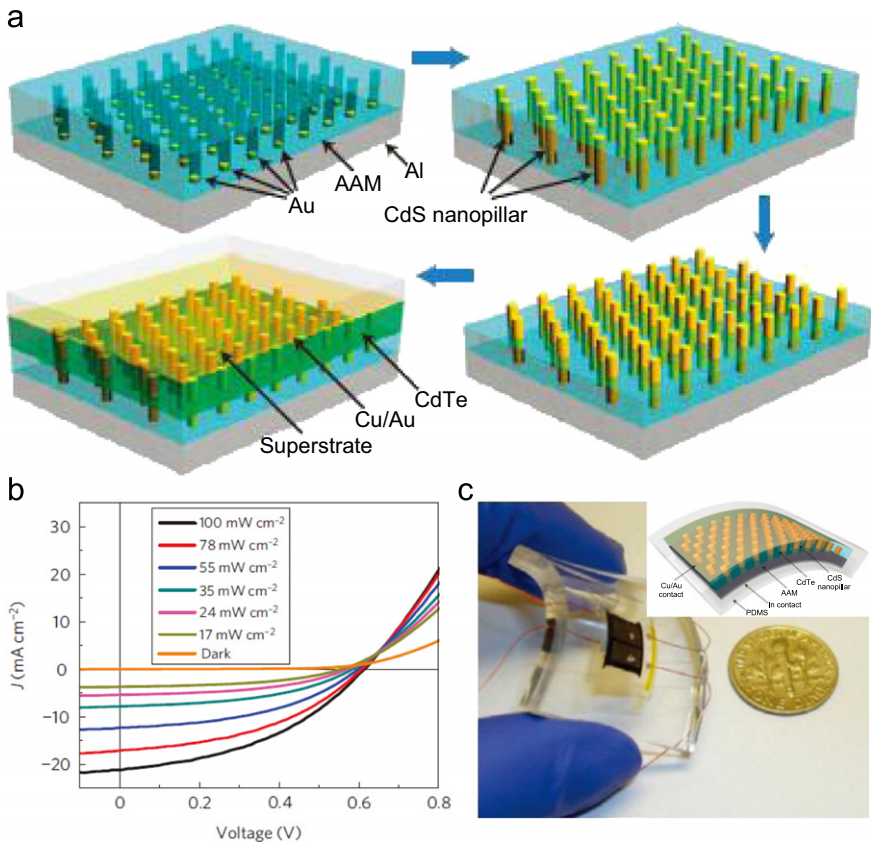

Figure 6 CdS NPLs/CdTe thin film PV devices. (a) Fabrication scheme of CdS NPLs/CdTe thin film cell. (b) *J*–*V* characteristics at different illumination intensities. (c) An optical image and schematic (inert) of a bendable module embedded in PDMS. Adapted with permission from Ref. [4].

discrete energy levels in QD greatly slow down the energy dissipation process, thus the extra energy of high energy excitons can be utilized to excite new excitons, as schematically shown in Fig. 7a and b.

The evidence of multiple-exciton generation process has been reported by several groups [63–70]. Schaller and Klimov first reported an excitation energy threshold for the formation of two or more excitons in PbSe nanocrystals (NC) when pump photon energies are more than 3 times the NCs band gap energy [64]. Ellingson et al. have reported quantum yield value of 300% for 3.9 nm diameter PbSe QDs at a photon energy of 4 times the QDs badgap, indicating the creation of three excitons per photon for every photo-excited QD [65]. More experimental investigations were also conducted by other groups on PbS QDs [65], PbTe QDs [67], CdSe QDs [71], Si QDs [70], and InP QDs [63].

In fact, research on how much the quantum confinement really enhances the MEG process has been the focus in the field of QD photovoltaics. According to recent study, the MEG rate increases as the QD volume decreases because of volume dependence, considering that Coulomb coupling and density of states do not cancel each other [72], as shown in Fig. 7c and d. Lin et al. argued that it is more appropriate to describe the trend of the MEG efficiency by calculations using fixed relative photon energy [72]. Otherwise, the opposite trend is found if the comparison is made using the absolute photon energy for each QD. Both the effective Coulomb coupling and the density of states are energy dependent, with the latter being a stronger function of energy [72].

Nanoparticle/QD PV devices

The most common approach to synthesize colloidal QDs is the controlled nucleation and growth of particles in a solution of chemical precursors containing inorganic salts or organometallic compounds. In the so-called hot-injection technique, the precursors are rapidly injected into a hot and vigorously stirred solvent containing organic surfactant molecules that can coordinate with the surface of the precipitated QD particles. This method is usually used to synthesize II–VI and I–VI semiconductor colloidal QD [56,58,73]. The organic surfactant molecules play the key role in tuning the kinetics of nucleation and growth by preventing or limiting particle growth via Ostwald ripening [10]. Following the similar growth process, a number of NCs have been synthesized, including CdS [74], CdTe [62], CdSe [58], Copper–Indium–Selenide [60,75,76], etc. And these NCs have been fabricated into PV devices [62,74]. In one of the pioneering works, Gur et al. introduced an ultrathin donor–acceptor solar cell composed entirely of inorganic NCs spin-cast from solution [62]. The NCs used in PV devices are rod-shaped CdSe (Fig. 8a) and CdTe (Fig. 8b) NCs prepared by air-free hot-injection techniques. In fabricating process, CdTe and CdSe NCs were first spin-cast onto ITO substrate to create ultrathin and compact film, and then sintered to minimize the high surface trap area inherent in a densely packed array of

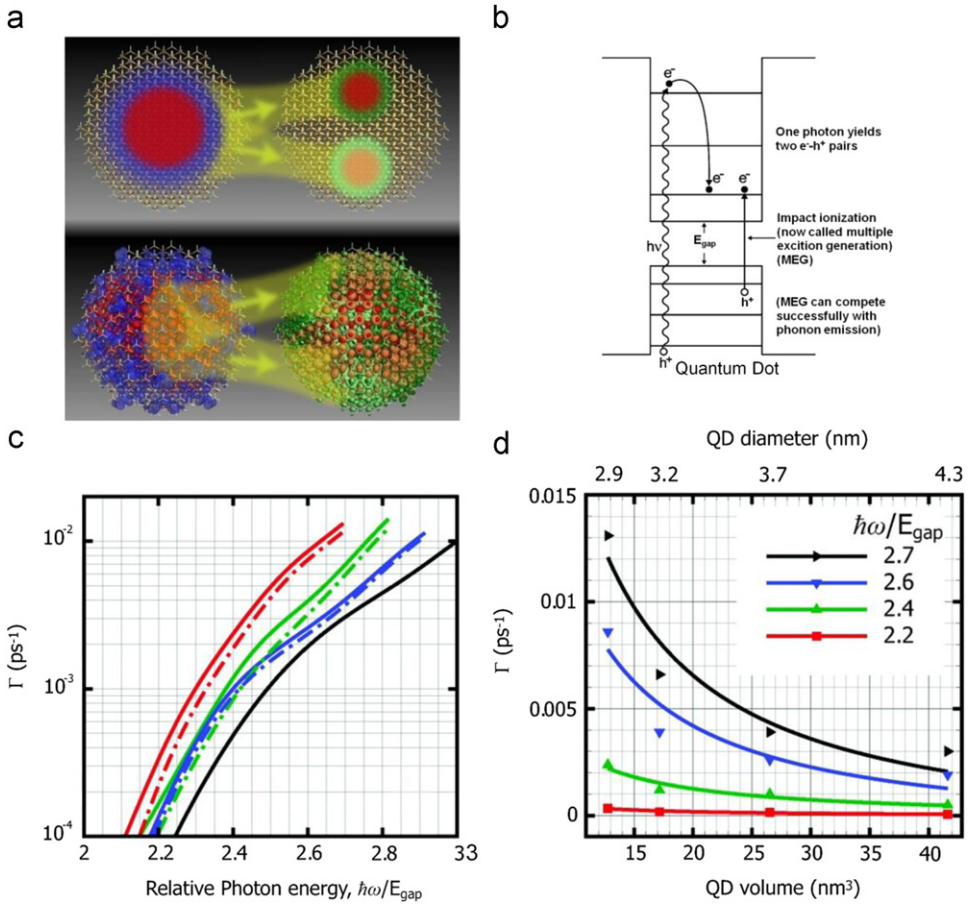

Figure 7 (a) In multiple-exciton generation (MEG) an exciton transfers energy to more than one electron. The left side shows an electron promoted to a high energy state (blue) plus the "hole" vacated by the electron (red). The right side shows the original exciton (now dark green/red) and a new exciton (light green/orange) after MEG. The top image shows a conceptualized version while the bottom shows an actual exciton and bi-exciton. Adapted with permission from Ref. [72]. (b) Multiple electron-hole pair (exciton) generation (MEG) in quantum dots. Adapted with permission from Ref. [10]. (c) MEG rate as a function of relative photon energy scaled by the optical band gaps for four CdSe QDs. (d) Volume dependence of the MEG rate of CdSe QDs, calculated at fixed relative photon energy scaled by the optical band gap. Adapted with permission from Ref. [72].

NCs as well as concurrently improve carrier transport in the device. With J_{sc} of 13.2 mA cm^{-2}, V_{oc} of 0.45 V, and FF of 0.49, the CdTe/CdSe bilayer solar cell demonstrated a power conversion efficiency of 2.9% under simulated AM1.5G illumination (Fig.8c). This demonstration elucidates a class of photovoltaic devices with potential for stable, low-cost power generation [62].

Besides the donor–acceptor solar cell, Luther et al. demonstrated an all-inorganic schottky junction metal/PbSe NC/metal sandwich photovoltaic (PV) cell, which can produce a J_{sc} larger than 21 mA cm^{-2} (Fig. 8d–f) [12]. Device fabrication was performed by depositing a 60–300 nm thick film of monodisperse, spheroidal PbSe NCs onto patterned indium tin oxide (ITO) coated glass, followed by evaporation of a top metal contact. The PV cell yields an external quantum efficiency of 55–65% in the visible and up to 25% in the infrared region of the solar spectrum, with a spectrally corrected AM1.5G power conversion efficiency of 2.1%. This NC device produces one of the largest short-circuit currents of any nanostructured solar cell, without the need for sintering, superlattice order or separate phases for electron and hole transport.

Other nanostructured solar cells

Above discussions have covered a number of major types nanostructures for PV studies, including NW, NR, NPL, NC/QDs, etc. These studies have been extensively reported in the field. On the other hand, due to the diversity of nanomaterial growth/fabrication processes, there are many other nanomaterials with unique geometry/structure, which can also be potentially utilized to fabricate efficient and low cost PV devices. These nanostructures include nanodisk [77], nanoflower [78], hierarchical nanowire [79–81], nanotetrapods [82], nanooctahedra [83], nanospindles [84], nanobamboo [85], hierarchical nanoplate [86] and nanobelt [87]. In this section, research on some of the unique structures, including nanodome [88], nanotube [89], nano-forest [90], etc., will be reviewed.

Novel silicon nanostructures: nanodome, nanohole solar cells

Nanoscale surface textures on solar cell surface enhance light scattering and absorption, besides using NW, NPL, etc.,

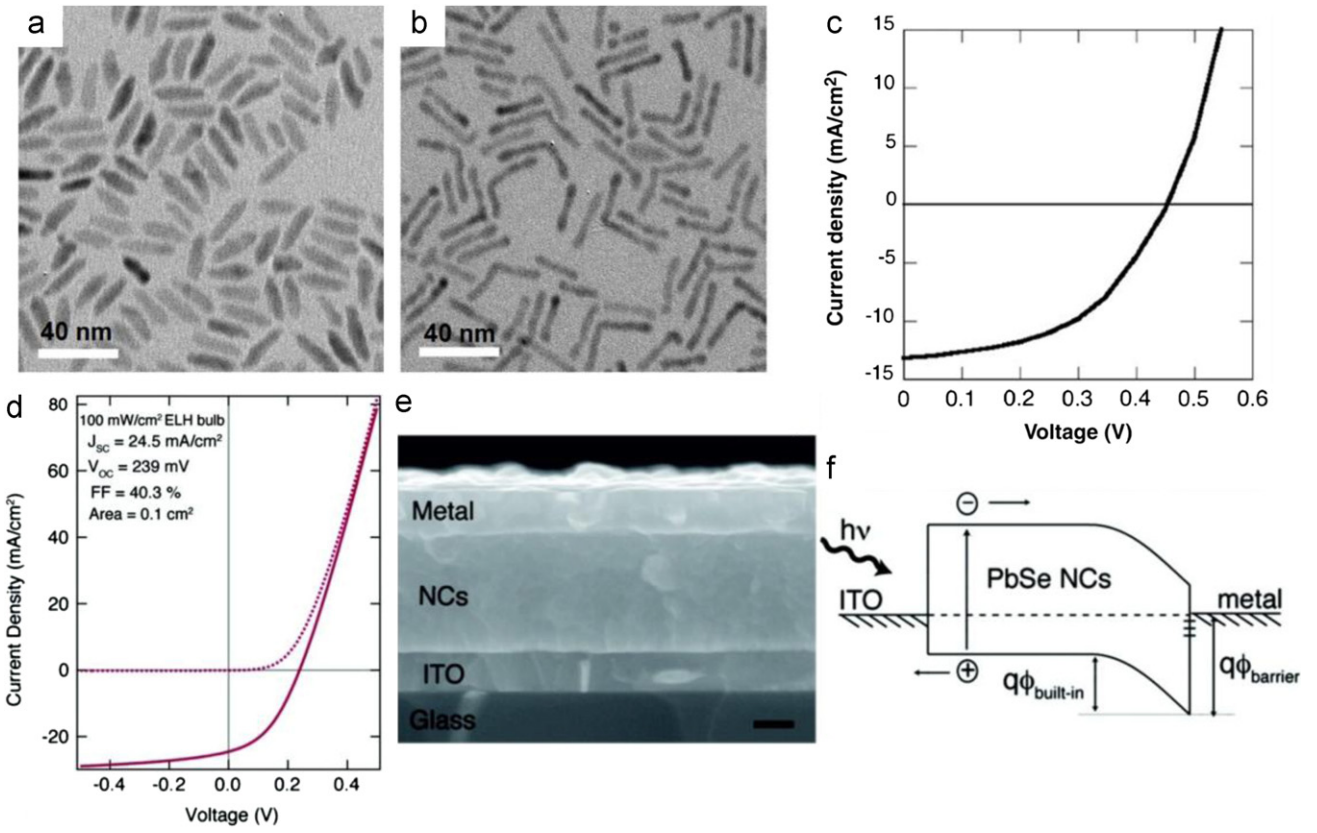

Figure 8 Transmission electron micrographs of (a) CdSe and (b) CdTe NCs. (c) *I-V* characteristics of a typical bilayer CdTe/CdSe device showing the efficiency of 2.9%. Adapted with permission from Ref. [62]. (d) *I-V* characteristic, (e) Structure, and (f) Schematic diagram of the PbSe solar cell device. Adapted with permission from Ref. [12].

to serve this purpose, nanodome structure was also fabricated on amorphous silicon solar cell, as shown in Fig. 9a [88]. Specifically, an array of nanodome was fabricated by Langmuir-Blodgett assembly of close packed monodisperse SiO_2 beads on a glass or quartz substrate, followed by reactive ion etching (RIE) resulting nanocone arrays on the substrate [6]. The nanocone substrate was then coated with 280nm thick hydrogenated amorphous silicon (a-Si:H) layer that can absorb 94% of the light within wavelength range of 400–800 nm shown by optical measurements [88]. This absorption capability is significantly higher than that of flat film devices, which is only 65% [88]. Enhanced light absorption can also be confirmed by much improved PV performance of nanodome solar cell. Fig. 9b shows the *I-V* characteristic of a nanodome solar cell showing V_{oc} of 0.75 V, J_{sc} of 17.5 mA cm^{-2} with a FF of 0.45 and efficiency of 5.9% [88]. This performance is much improved as compared to a flat control sample, which has V_{oc} of 0.76 V, J_{sc} of 11.4 mA cm^{-2}, FF of 0.54 and efficiency of 4.7% [88]. Furthermore, surface of this nanodome structure was found to be superhydrophobic after modified with hydrophobic molecule perfluorooctyl trichlorosilane (PFOS) and with a contact angle about 150° [88]. This unique feature indicates that nanodome solar cells can have self-cleaning function, suitable for installation in dusty environment.

As have shown so far, Si based nanostructures for light trapping and solar cells have been widely studied, mainly due to the fact that Si is still the dominant materials for semiconductor and photovoltaic industry. One thing in common for the aforementioned nanostructures, including, NWs, MWs, NPLs, is that these structures are all positive structures relative to substrate. In fact, light trapping can be also performed efficiently with complementary negative structures, such as nanopores and nanoholes [17]. In this regard, Peng et al. fabricated nanohole arrays on Si wafer with photolithography and metal-assisted etching [20]. After fabrication of the holes, radial *p–n* junctions on the side walls of the nanoholes were formed by gas phase thermal phosphorus dopant diffusion, as shown in Fig. 9c [20]. PV performance characterization (Fig. 9d) has shown such a nanohole solar cell can achieve 9.51% conversion efficiency, which is better than the planar control sample and the sample with pyramids surface texture [20]. This result confirmed the theoretical analysis done by Han and Chen reviewed in Section 2.1 of this article [17]. In addition, such a nanohole geometry exhibits superior mechanical robustness in comparison with the fragile structure of the free-standing nanowire radial *p–n* junction solar cell.

Nanotube and nano-forest dye-sensitized solar cells (DSSCs)

The above reviewed nanomaterial/nanostructures are primarily for *p–n* junction inorganic PV. As a matter of fact, nanostructures are also widely used as photoanodes of dye-sensitized solar cells (DSSCs) [78,80,82,84,85,89–99]. In this

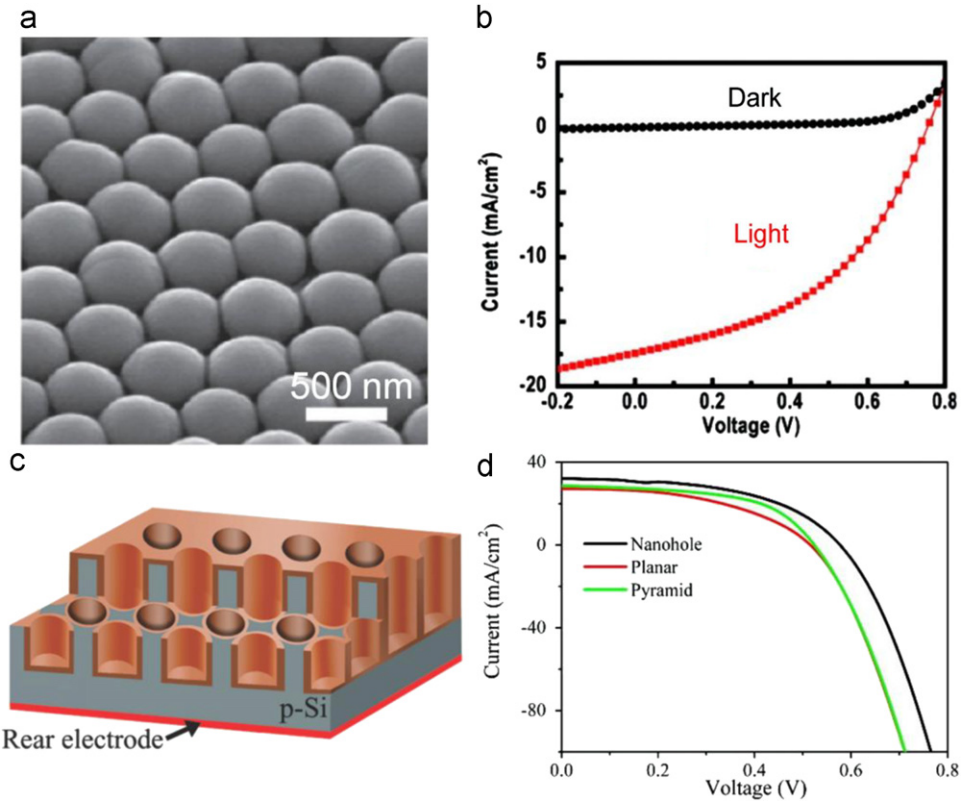

Figure 9 (a) a-Si:H nanodome solar cells deposited on nanocones substrate. (b) Dark and light *I*–*V* curve of nanodome solar cell. Adapted with permission from Ref. [88]. (c) Schematic cross-section of the Si nanohole solar cell with radial *p*-*n* junctions, the *n*+ layer is shown in purple bronze, the p-Si substrate in gray, and the rear electrode in red. (d) *I*–*V* curves for solar cells with different geometries. Adapted with permission from Ref. [20].

case large surface area of nanostructures is utilized for high dye loading and electrolyte absorption. In the following paragraphs, a few examples of DSSC based on nanostructures will be briefly introduced.

One of the pioneering works on nanostructured DSSC was performed with ZnO NWs demonstrating ~1.2% conversion efficiency [100]. Ever since then a number of research groups have explored a variety of nanostructures achieving progressively improved conversion efficiencies [78,83]. Fig. 10a shows a schematic of anodic titanium oxide (ATO) nanotube based DSSC device [89]. ATO fabrication is well-established and the tubular structure can increase the electron diffusion length to the order of 100 μm leading to efficient charge separation [89]. Initial test showed that this type of solar cell can deliver 2.9% efficiency, as shown in Fig. 10b. It was found that one of the performance limiting factors is the relatively high resistivity of TiO_2 nanotube matrix especially the tube bottom which leads to suppressed fill factor [89]. Therefore a reduction process was performed to convert Ti^{4+} ions to Ti^{3+} ions. The Ti^{3+} ions served as donors and increased the conductivity of barrier layer. With this process, the conversion efficiency was improved to ~3.9%, as shown in Fig. 10b.

The main advantage of using nanostructures for DSSC rests in their large surface area, therefore researchers are actively exploring fabrication of hierarchical nanostructures and their applications in PV devices. Fig. 10c shows a schematic and SEM image of ZnO nano-forest synthesized by low cost hydrothermal method [90]. Obviously such a structure provides extremely large surface area for dye adsorption. In fact, the researchers have fabricated 6 different ZnO nanostructures, ranging from NWs (LG1) to nano-forest (BG3), with increasing degree of hierarchy and surface area for each structure, namely from LG1, LG2, and LG3 to BG1, BG2 and BG3, respectively [90]. Interestingly, electrical characterization showed that short circuit current density of the solar cells increased generally with increasing degree of hierarchy, as shown in Fig. 10. Meanwhile, it was also pointed out that high density network of crystalline ZnO NWs can improve carrier extraction, and branched NWs can increase light-harvesting efficiency by introducing light scattering [90].

Besides the nanostructures briefly discussed in the section, there are many more nanostructures, such as nano-tetrapod [82], nanooctahedra[83], nanodisk [77], nano-bamboo [85], etc., have been explored for DSSC devices which cannot be elaborated in this review due to the page limit. Nevertheless, it is noteworthy that using nanomaterials for DSSC can not only improve the performance of devices, but also reduce the fabrication cost, as many nanomaterial processes are compatible with spin-coating, ink-jet printing, etc. These advantages can potentially lead to cost-effective PV technologies.

Hybrid nanostructure solar cell

In the above review, 3-D nanostructures have been proven efficient for both photon capturing and photo-carrier collection. It is worth noting that in most cases photons

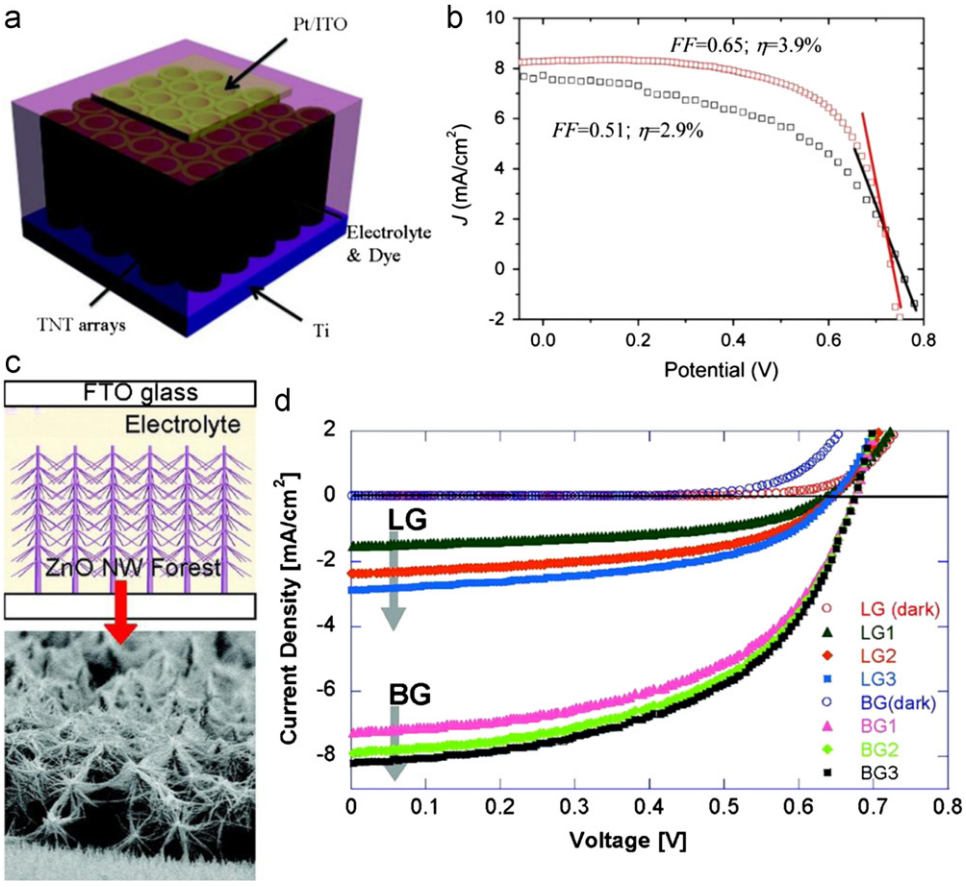

Figure 10 (a) Schematic of ATO nanotubes-based DSSC. (b) *J–V* characteristics of DSSCs with (red) and without (black) bottom reductive doping treatment. Adapted with permission from Ref. [89]. (c) Schematic (top) and SEM micrograph (bottom) of nanotree and nanoforest structure. (d) *J–V* curve of dye-sensitized solar cell with nano-forest ZnO NW. Adapted with permission from Ref. [90].

are captured after traveling across free space when they enter the 3-D structure, therefore, in order to achieve efficient light absorption the entire 3-D structure needs to be exposed directly under sunlight. In a non-conventional and innovative design, ZnO NWs were integrated with an optical waveguide, as shown in Fig. 11a and b [93]. In such a hybrid 3-D design, the ZnO NWs was grown normally to the optical fiber surface and light was guided into optical fiber by illuminating the fiber from either one exposed side of the fiber so that incident light is normal to fiber axis (NA, Fig. 11c), or one end along the axial direction (PA, Fig. 11c). In experiments, DSSC solar cells were fabricated based on these two configurations [93]. Electrical measurements have shown that although the NA case showed slightly higher V_{oc} than the PA case due to uniformly high light intensity at ZnO-dye interface, J_{sc} of PA case is more than 3 $\times$ of that of NA case, due to the efficiency light trapping inside the fiber [93]. Taking into account the improved fill factor for PA case, eventually, efficiency of PA case (3.3%) is nearly 4 $\times$ of that of NA case (0.76%) [93]. This interesting work suggests that although a conventional optical component, such as optical fiber, is usually designed as a low loss device to guide photon to travel across long distance, once combining with nanomaterials for solar cell application, its waveguding property becomes excellent light trapping mechanism.

Conclusions and future perspectives

This review article provides a comprehensive summary of state-of-art research on nanomaterials/nanostructures based photovoltaics. The main motivations of the research in this field originate from several advantages of nanomaterials/nanostructures, as compared to their thin film/bulk counterparts. These include significantly improved photon capturing and photo-carrier collection capability, potential new photovoltaic mechanism exceeding current thermodynamic limits, as well as low cost and scalable processes. Well integrating all these positive aspects together, it is likely to deliver a new generation of photovoltaics with attractive cost-effectiveness. As the family of nanomaterials has great diversity, we highlighted a number of materials and structures being widely studied, including nanowires, nanopillars, nanocones, nanodomes, nanoparticles, etc. And we have covered materials include crystalline Si, amorphous Si, CdS, CdSe, CdTe, ZnO, CIS, etc. These materials and structures have different physical properties, such as band-gap, absorption coefficient, surface/bulk recombination rate, etc., as well as different synthesis/fabrication approaches. Overall, these inorganic materials have much better stability than organic materials thus they can meet the expectation for longer device life-time as compared to

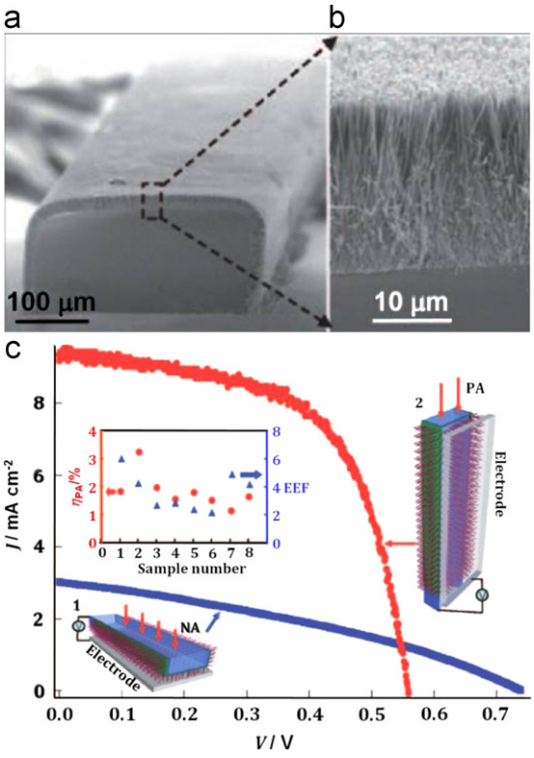

Figure 11 (a) Low-magnification SEM micrograph of a quartz optical fiber with uniformly grown ZnO NWs on three sides. (b) High-magnification SEM micrograph showing the densely packed ZnO NWs on the fiber surface (c) *J*–*V* curves of a DSSC under one full-sun AM1.5G illumination oriented case (1) normal to the fiber axis and case (2) parallel to the fiber axis. Adapted with permission from Ref. [93].

organic photovoltaics. It is worth noting that up to date, the performance of nanostructured photovoltaic devices has not surpassed the records of the bulk/thin film devices made of the same materials. And the bottleneck challenge rests in large surface area causing increased surface recombination, as compared to planar bulk/thin film devices. To relieve the effect of surface recombination on device performance, geometrical design of nanostructures have to be optimized in the first place to take advantage of light trapping and carrier collection enhancement without significant increase of surface recombination. On the other hand, surface passivation technique can be applied on nanostructures to reduce surface recombination. It is known to all that the ultimate photovoltaic technology needs to be high efficiency, low cost, and environmental friendly. Depend on applications, addition requirements such as flexibility, portability, etc., are also expected. It is out of question that nanomaterials based photovoltaics have potency to address these needs, and with the enormous effort being invested, progress will be made continuously in the future.

Acknowledgment

Q. Lin and S.F. Leung acknowledge partial support by National Research Foundation of Korea funded by the Korean Government (NRF-2010-220-D00060).

References

[1] K. Palmer, D. Burtraw, Energy Economics 27 (2005) 873.
[2] E.C. Garnett, P.D. Yang, Nano Letters 10 (2010) 1082.
[3] B.D. Yuhas, P. Yang, Journal of the American Chemical Society 131 (2009) 3756.
[4] Z.Y. Fan, H. Razavi, J.W. Do, A. Moriwaki, O. Ergen, Y.L. Chueh, P.W. Leu, J.C. Ho, T. Takahashi, L.A. Reichertz, S. Neale, K. Yu, M. Wu, J.W. Ager, A. Javey, Nature Materials 8 (2009) 648.
[5] K. Cho, D.J. Ruebusch, M.H. Lee, J.H. Moon, A.C. Ford, R. Kapadia, K. Takei, O. Ergen, A. Javey, Applied Physics Letters 98 (2011) 203101.
[6] J. Zhu, Z.F. Yu, G.F. Burkhard, C.M. Hsu, S.T. Connor, Y.Q. Xu, Q. Wang, M. McGehee, S.H. Fan, Y. Cui, Nano Letters 9 (2009) 279.
[7] B.M. Kayes, H.A. Atwater, N.S. Lewis, Journal of Applied Physics 97 (2005) 114302.
[8] Z.Y. Fan, R. Kapadia, P.W. Leu, X.B. Zhang, Y.L. Chueh, K. Takei, K. Yu, A. Jamshidi, A.A. Rathore, D.J. Ruebusch, M. Wu, A. Javey, Nano Letters 10 (2010) 3823.
[9] L.K. Yeh, K.Y. Lai, G.J. Lin, P.H. Fu, H.C. Chang, C.A. Lin, J.H. He, Advanced Energy Materials 1 (2011) 506.
[10] A.J. Nozik, M.C. Beard, J.M. Luther, M. Law, R.J. Ellingson, J.C. Johnson, Chemical Review 110 (2010) 6873.
[11] D.V. Talapin, J.S. Lee, M.V. Kovalenko, E.V. Shevchenko, Chemical Reviews 110 (2010) 389.
[12] J.M. Luther, M. Law, M.C. Beard, Q. Song, M.O. Reese, R.J. Ellingson, A.J. Nozik, Nano Letters 8 (2008) 3488.
[13] E.D. Kosten, E.L. Warren, H.A. Atwater, Optical Express 19 (2011) 3316.
[14] H. Sai, M. Kondo, Solar Energy Materials and Solar Cells 95 (2010) 131.
[15] M.D. Kelzenberg, S.W. Boettcher, J.A. Petykiewicz, D.B. Turner-Evans, M.C. Putnam, E.L. Warren, J.M. Spurgeon, R.M. Briggs, N.S. Lewis, H.A. Atwater, Nature Materials 9 (2010) 239.
[16] L. Hu, G. Chen, Nano Letters 7 (2007) 3249.
[17] S.E. Han, G. Chen, Nano Letters 10 (2010) 1012.
[18] S.E. Han, G. Chen, Nano Letters 10 (2010) 4692.
[19] E.C. Greyson, Y. Babayan, T.W. Odom, Advanced Materials 16 (2004) 1348.
[20] K. Peng, X. Wang, L. Li, X. Wu, S. Lee, Journal of the American Chemical Society 132 (2010) 6872.
[21] W.K. Choi, T.H. Liew, M.K. Dawood, H.I. Smith, C.V. Thompson, M.H. Hong, Nano Letters 8 (2008) 3799.
[22] Y. Wu, Y. Cui, L. Huynh, C.J. Barrelet, D.C. Bell, C.M. Lieber, Nano Letters 4 (2004) 433.
[23] Y.Y. Wu, P.D. Yang, Journal of the American Chemical Society 123 (2001) 3165.
[24] D.E. Perea, N. Li, R.M. Dickerson, A. Misra, S.T. Picraux, Nano Letters 11 (2011) 3117.
[25] V. Schmidt, S. Senz, U. Gösele, Nano Letters 5 (2005) 931.
[26] T. Kuykendall, P.J. Pauzauskie, Y. Zhang, J. Goldberger, D. Sirbuly, J. Denlinger, P. Yang, Nature Materials 3 (2004) 524.
[27] H.J. Fan, F. Bertram, A. Dadgar, J. Christen, A. Krost, M. Zacharias, Nanotechnology 15 (2004) 1401.
[28] Z.L. Wang, X.Y. Kong, Y. Ding, P. Gao, W.L. Hughes, R. Yang, Y. Zhang, Advanced Functional Materials 14 (2004) 943.
[29] C.R. Martin, Chemistry of Materials 8 (1996) 1739.
[30] D. Xu, Y. Xu, D. Chen, G. Guo, L. Gui, Y. Tang, Advanced Materials 12 (2000) 520.
[31] Y.L. Chueh, Z.Y. Fan, K. Takei, H. Ko, R. Kapdia, A. Rathore, N. Miller, K. Yu, M. Wu, E.E. Haller, A. Javey, Nano Letters 10 (2010) 520.
[32] O. Ergen, D.J. Ruebusch, H. Fang, A.A. Rathore, R. Kapadia, Z. Fan, K. Takei, A. Jamshidi, M. Wu, A. Javey, Journal of the American Chemical Society 132 (2010) 13972.
[33] K. Peng, A. Lu, R. Zhang, S.T. Lee, Advanced Functional Materials 18 (2008) 3026.

[34] J.M. Spurgeon, H.A. Atwater, N.S. Lewis, Jounal of Physical Chemistry C 112 (2008) 6186.
[35] B.Z. Tian, X.L. Zheng, T.J. Kempa, Y. Fang, N.F. Yu, G.H. Yu, J.L. Huang, C.M. Lieber, Nature 449 (2007) 885.
[36] T.J. Kempa, B. Tian, D.R. Kim, J. Hu, X. Zheng, C.M. Lieber, Nano Letters 8 (2008) 3456.
[37] Z. Fan, D.J. Ruebusch, A.A. Rathore, R. Kapadia, O. Ergen, P.W. Leu, A. Javey, Nano Research 2 (2009) 829.
[38] M.C. Putnam, D.B. Turner-Evans, M.D. Kelzenberg, S.W. Boettcher, N.S. Lewis, H.A. Atwater, Applied Physics Letters 95 (2009) 163116.
[39] M.D. Kelzenberg, D.B. Turner-Evans, M.C. Putnam, S.W. Boettcher, R.M. Briggs, J.Y. Baek, N.S. Lewis, H.A. Atwater Energy and Environmental Science 4 (2011) 866.
[40] J. Tang, Z. Huo, S. Brittman, H. Gao, P. Yang, Nature Nanotechnology 6 (2011) 568.
[41] X.F. Duan, C.M. Lieber, Advanced Materials 12 (2000) 298.
[42] J.A. Bragagnolo, A.M. Barnett, J.E. Phillips, R.B. Hall, A. Rothwarf, J.D. Meakin, IEEE Transactions on Electron Devices 27 (1980) 645.
[43] C. Colombo, M. Heiss, M. Gratzel, A.F.I. Morral, Applied Physics Letters 94 (2009) 173108.
[44] M.S. Islam, H. Ishino, T. Kawano, H. Takao, K. Sawada, M. Ishida, Japanese Journal of Applied Physics 44 (2005) 2161.
[45] T. Yanagida, A. Marcu, H. Matsui, K. Nagashima, K. Oka, K. Yokota, M. Taniguchi, T. Kawai, Jounal of Physical Chemistry C 112 (2008) 18923.
[46] Y. Yan, L. Zhou, J. Zhang, H. Zeng, Y. Zhang, L. Zhang, Jounal of Physical Chemistry C 112 (2008) 10412.
[47] D.R. Kim, C.H. Lee, P.M. Rao, I.S. Cho, X.L. Zheng, Nano Letters 11 (2011) 2704.
[48] E.C. Garnett, P.D. Yang, Journal of the American Chemical Society 130 (2008) 9224.
[49] B.M. Kayes, M.A. Filler, M.C. Putnam, M.D. Kelzenberg, N.S. Lewis, H.A. Atwater, Applied Physics Letters 91 (2007) 103110.
[50] R. Kapadia, Z. Fan, A. Javey, Applied Physics Letters 96 (2010) 103116.
[51] A.J. Sabbah, D.M. Riffe, Journal of Applied Physics 88 (2000) 6954.
[52] M.W. Rowe, H.L. Liu, G.P. Williams, R.T. Williams, Physical Review B 47 (1993) 2048.
[53] A.K. Sharma, S.K. Agarwal, S.N. Singh, Solar Energy Materials and Solar Cells 91 (2007) 1515.
[54] Y. Rosenwaks, L. Burstein, Y. Shapira, D. Huppert, Applied Physics Letters 57 (1990) 458.
[55] I. Delgadillo, M. Vargas, A. CruzOrea, J.J. Alvarado-Gil, R. Baquero, F. Sanchez-Sinencio, H. Vargas, Applied Physics B 64 (1997) 97.
[56] Z.A. Peng, X. Peng, Journal of the American Chemical Society 123 (2001) 183.
[57] X. Peng, J. Wickham, A.P. Alivisatos, Journal of the American Chemical Society 120 (1998) 5343.
[58] A.L. Rogach, D.V. Talapin, E.V. Shevchenko, A. Kornowski, M. Haase, H. Weller, Advanced Functional Materials 12 (2002) 653.
[59] C.R. Corwine, A.O. Pudov, M. Gloeckler, S.H. Demtsu, J.R. Sites, Solar Energy Materials and Solar Cells 82 (2004) 481.
[60] W.W. Hou, B. Bob, S. Li, Y. Yang, Thin Solid Films. 517 (2009) 6853.
[61] W. Shockley, H.J. Queisser, Journal of Applied Physics 32 (1961) 510.
[62] I. Gur, N.A. Fromer, M.L. Geier, A.P. Alivisatos, Science 310 (2005) 462.
[63] S.K. Stubbs, S.J.O. Hardman, D.M. Graham, B.F. Spencer, W.R. Flavell, P. Glarvey, O. Masala, N.L. Pickett, D.J. Binks, Physical Review B 81 (2010) 081303.
[64] R.D. Schaller, V.I. Klimov, Physical Review Letters 92 (2004) 186601.
[65] R.J. Ellingson, M.C. Beard, J.C. Johnson, P. Yu, O.I. Micic, A.J. Nozik, A. Shabaev, A.L. Efros, Nano Letters 5 (2005) 865.
[66] D. Gachet, A. Avidan, I. Pinkas, D. Oron, Nano Letters 10 (2009) 164.
[67] J.E. Murphy, M.C. Beard, A.G. Norman, S.P. Ahrenkiel, J.C. Johnson, P. Yu, O.I. Micic, R.J. Ellingson, A.J. Nozik, Journal of the American Chemical Society 128 (2006) 3241.
[68] R.D. Schaller, M. Sykora, S. Jeong, V.I. Klimov, Journal of Physical Chemistry B 110 (2006) 25332.
[69] J.J.H. Pijpers, E. Hendry, M.T.W. Milder, R. Fanciulli, J. Savolainen, J.L. Herek, D. Vanmaekelbergh, S. Ruhman, D. Mocatta, D. Oron, Jounal of Physical Chemistry C 111 (2007) 4146.
[70] M.C. Beard, K.P. Knutsen, P.R. Yu, J.M. Luther, Q. Song, W.K. Metzger, R.J. Ellingson, A.J. Nozik, Nano Letters 7 (2007) 2506.
[71] R.D. Schaller, M.A. Petruska, V.I. Klimov, Applied Physics Letters 87 (2005) 253102.
[72] Z. Lin, A. Franceschetti, M.T. Lusk, ACS Nano 5 (2010) 2503.
[73] M. Kar, R. Agrawal, H.W. Hillhouse, Journal of the American Chemical Society. (2011) (Article ASAP).
[74] L. Li, X. Yang, J. Gao, H. Tian, J. Zhao, A. Hagfeldt, L. Sun, Journal of the American Chemical Society 133 (2011) 8458.
[75] Q. Guo, S.J. Kim, M. Kar, W.N. Shafarman, R.W. Birkmire, E.A. Stach, R. Agrawal, H. Hillhouse, Nano Letters 8 (2008) 2982.
[76] D.B. Mitzi, M. Yuan, W. Liu, A.J. Kellock, S.J. Chey, V. Deline, A.G. Schrott, Advanced Materials 20 (2008) 3657.
[77] J.X. Wang, C.M.L. Wu, W.S. Cheung, L.B. Luo, Z.B. He, G.D. Yuan, W.J. Zhang, C.S. Lee, S.T. Lee, Jounal of Physical Chemistry C 114 (2010) 13157.
[78] C.Y. Jiang, X.W. Sun, G.Q. Lo, D.L. Kwong, J.X. Wang, Applied Physics Letters 90 (2007) 263501.
[79] D.I. Suh, S.Y. Lee, T.H. Kim, J.M. Chun, E.K. Suh, O.B. Yang, S.K. Lee, Chemical Physics Letters 442 (2007) 348.
[80] H. Cheng, W. Chiu, C. Lee, S. Tsai, W. Hsieh, Jounal of Physical Chemistry C 112 (2008) 16359.
[81] J. Oh, J. Lee, H. Kim, S. Han, K. Park, Chemistry of Materials 22 (2010) 1114.
[82] W. Chen, Y. Qiu, Y. Zhong, K.S. Wong, S. Yang, Journal of Physical Chemistry A 114 (2010) 3127.
[83] K. Yan, Y. Qiu, W. Chen, M. Zhang, S. Yang, Energy and Environmental Science 4 (2011) 2168.
[84] Y. Qiu, W. Chen, S. Yang, Angewandte Chemie International Edition 49 (2010) 3675.
[85] D. Kim, A. Ghicov, S.P. Albu, P. Schmuki, Journal of the American Chemical Society 130 (2008) 16454.
[86] Y. Qiu, W. Chen, S. Yang, Journal of Materials Chemistry 20 (2010) 1001.
[87] C. Lin, H. Lin, J. Li, X. Li, Journal of Alloys and Compounds 462 (2008) 175.
[88] J. Zhu, C. Hsu, Z. Yu, S. Fan, Y. Cui, Nano Letters 10 (2010) 1979.
[89] D. Li, P. Chang, C. Chien, J.G. Lu, Chemistry of Materials 22 (2010) 5707.
[90] S.H. Ko, D. Lee, H.W. Kang, K.H. Nam, J.Y. Yeo, S.J. Hong, C.P. Grigoropoulos, H.J. Sung, Nano Letters 11 (2011) 666.
[91] M. Law, L.E. Greene, J.C. Johnson, R. Saykally, P.D. Yang, Nature Materials 4 (2005) 455.
[92] M. Adachi, Y. Murata, J. Takao, J.T. Jiu, M. Sakamoto, F.M. Wang, Journal of the American Chemical Society 126 (2004) 14943.
[93] B. Weintraub, Y. Wei, Z.L. Wang, Angewandte Chemie International Edition 48 (2009) 8981.

[94] A.B.F. Martinson, J.W. Elam, J. Liu, M.J. Pellin, T.J. Marks, J.T. Hupp, Nano Letters 8 (2008) 2862.
[95] K. Zhu, N.R. Neale, A. Miedaner, A.J. Frank, Nano Letters 7 (2007) 69.
[96] J.B. Baxter, E.S. Aydil, Solar Energy Materials and Solar Cells 90 (2006) 607.
[97] Y. Chiba, A. Islam, Y. Watanabe, R. Komiya, N. Koide, L. Han, Japanese Journal of Applied Physics 45 (2006) L638.
[98] M. Law, L.E. Greene, A. Radenovic, T. Kuykendall, J. Liphardt, P.D. Yang, Journal of Physical Chemistry B 110 (2006) 22652.
[99] G. Mor, K. Shankar, M. Paulose, O. Varghese, C. Grimes, Nano Letters 6 (2006) 215.
[100] L.E. Greene, B.D. Yuhas, M. Law, D. Zitoun, P. Yang, Inorganic Chemistry 45 (2006) 7535.

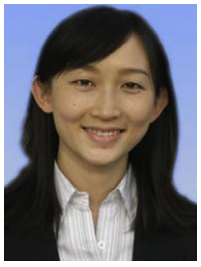

Rui Yu received her B.S. degree in Material Science and Engineering from Tongji University in 2003, and Ph.D. degree in Physical Chemistry from Dalian Institute of Chemical Physics, Chinese Academy of Science in China in 2010. She joined Prof. Zhiyong Fan's research group at Hong Kong University of Science and Technology as a postdoctoral researcher since September 2010. Her current research interests focus on the novel nanostructured materials for photovoltaic applications.

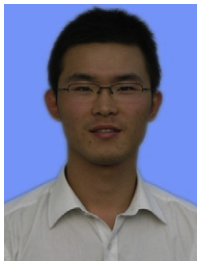

Qingfeng Lin is a Ph.D. student in Department of Electronic and Computer Engineering in the Hong Kong University of Science and Technology. He received his B.S. degree in Electronic Science and Technology from University of Science and Technology of China. His current research interests focus on the fabrication of nanostructures with self-organized approaches for photonic and electronic applications.

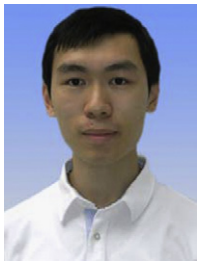

Siu-Fung Leung received his bachelor degree in Materials Engineering at City University of Hong Kong, and currently he is a graduate student in Department of Electronics and Computer Engineering of Hong Kong University of Science and Technology. His research interest is on functional nanomaterials and their applications in photovoltaic and nano-electronic devices.

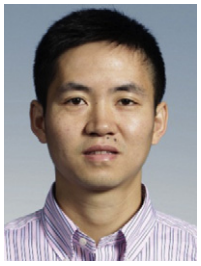

Zhiyong Fan received his B.S. and M.S. degrees in Physical Electronics from Fudan University, Shanghai, China, in 1998 and 2001. He received Ph.D. degree in Materials Science from University of California, Irvine in 2006. From 2007 to 2010, he worked in University of California, Berkeley as a postdoctoral fellow in Department of Electrical Engineering and Computer Sciences, with a joint appointment with Lawrence Berkeley National Laboratory. In May 2010, he joined Hong Kong University of Science and Technology as an assistant professor. His research interests include engineering novel nanostructures with functional materials, for technological applications including energy conversion, electronics and sensors, etc.